



	<b>Experiment title:</b> XEOL and $\mu$ Laue measurements of perovskite monocrystals for X-ray detection: materials and operando photocurrent	<b>Experiment number:</b> MA4957
<b>Beamline:</b> BM32	<b>Date of experiment:</b> from: 05 to 09 november 2021 reported to 01 to 04 april 2022	<b>Date of report:</b> 14/02/2023
<b>Shifts:</b> 9	<b>Local contact(s):</b> Jean-Sebastien MICHA; Olivier ULRICH;	<i>Received at ESRF:</i> 14/02/2023
<b>Names and affiliations of applicants</b> (* indicates experimentalists): Eric GROS-DAILLON <sup>1*</sup> ;  Ferdinand LÉDÉE <sup>1*</sup> ; Javier MAYEN <sup>2</sup> ; Jean-Marie VERILHAC <sup>2</sup> ;  Joel EYMERY <sup>3*</sup> ;  1 Univ. Grenoble Alpes, CEA, LETI, DOPT, F38000 Grenoble, France 2 Univ. Grenoble Alpes, CEA, LITEN, DTNM, F38000 Grenoble, France 3 Univ. Grenoble Alpes, CEA, IRIG, MEM, NRX, F38000 Grenoble, France		

### Report:

Thick layer of halide perovskite are studied as direct radiation detectors for medical X-ray radiography. Among these materials, methylammonium lead bromide single crystals are used as a model case to understand the charge carrier transport properties in this family of semiconductor material. The basic ideas of the proposal were:

1/ to correlate the crystalline quality to the optical emission of  $\text{CH}_3\text{NH}_3\text{PbBr}_3$  ( $\text{MAPbBr}_3$ ) hybrid perovskite crystals used for direct X-ray detection.

2/ to measure the photocurrent in top-view and cross-section configuration taking advantage of the small X-ray beam. In the cross-section geometry, the variation of the generated current, diffraction, and light give access to the photocurrent density as a function of the position of irradiation, and its defect dependence.

These operando measurements were enabled by the combination of XEOL which provide information on radiative recombination of the carriers with the  $\mu$ Laue structural analysis to measure the strain and tilt on the French CRG-IF BM32@ESRF beamline. This line provides a focused beam of size less than  $1\ \mu\text{m}$  and energy between 8 and 20keV. These two measurements were made at the same time as the transport of the charge carriers' evaluation by X-ray induced photocurrent.

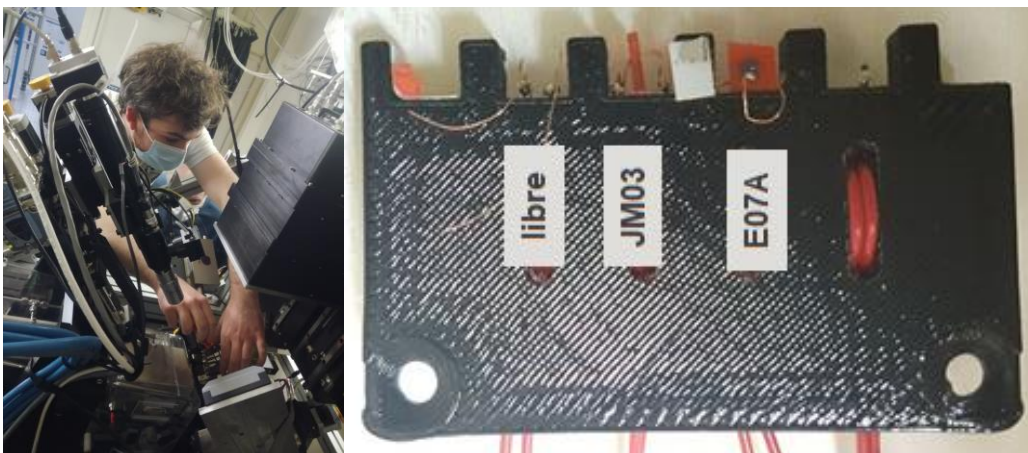


Figure 1 : Left: test environment. Right: example of measured samples

X-ray exposure demonstrated that samples were quickly damaged by the synchrotron beam. The luminescence was quenched very quickly under irradiation until disappearing completely. As an example, a first measurement of XEOL was performed on a small scanning area of  $3\times 3\mu\text{m}$ , then, a second measurement was performed on a larger scanning area of  $25\times 25\mu\text{m}$ , with the previous small area in the centre. The area irradiated during the first small scan of  $3\times 3\mu\text{m}$  appears darker in the second  $25\times 25\mu\text{m}$  scan. The fluorescence has declined on this area but appears exacerbated around (white halo). This increase in luminescence may be due to an increase in emitted XEOL intensity, or to a slight shift (1-2nm) of this luminescence towards low energies, where the perovskite reabsorbs less of its own luminescence, as shown in the luminescence curves and transmittance (see Figure 2). This experiment has been repeated (figure 2 central). In this repetition, a metallic electrode can be seen in black, without any luminescence as expected. These data were acquired on four different MAPbBr<sub>3</sub> single crystal samples. As an example, shown in Fig; 2, we compared the luminescence spectra for excitations at 400 nm visible light (black), 20 kV X-ray generator (green) and BM32 synchrotron source (blue) respectively. The red curve shows the transmitted spectrum in the visible range. All the curves are normalized for readability. The majority of the luminescence (black curve) is filtered by the perovskite itself. The low energy luminescence  $>560\text{ nm}$  that can be recorded with X-rays excitation (green and blue) comes from the bulk of the crystals whereas the higher energy luminescence ( $\sim 520\text{ nm}$ ) could only escape from the crystal surface when the crystals is excited with visible light. Only a small fraction of the generated luminescence can escape from the crystals, which results in a quite low XEOL intensity signal.

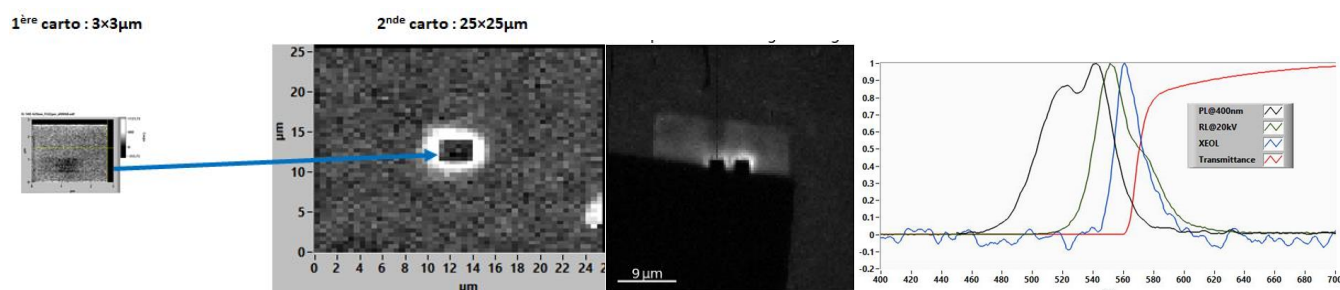
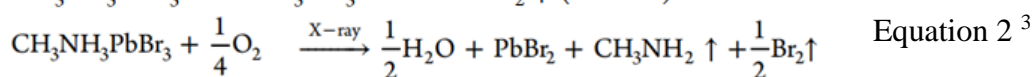
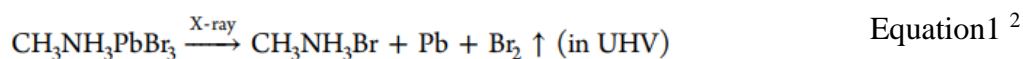


Figure 2 : Left, mapping of integrated XEOL between 500nm and 620nm. On the right, comparison of the luminescence measured by XEOL with the photoluminescence induced by visible photons and 20keV X-ray. A transmittance curve is added on this graph.

The observed extinction of luminescence could be attributed to the photodegradation of the perovskite. Two mechanisms are possible depending on the environmental conditions. In vacuum, the absorption of X-rays induces a decomposition of the perovskite into MABr, metallic lead and dibromium gas (equation 1). In air, the presence of oxygen induces a similar decomposition with the formation of water, lead dibromide, and methylamine and dibromium gas (equation 2). In both cases, the gaseous dibromine can escape from the perovskite and would cause irreversible degradation of the perovskite by loss of material. The highly irradiated samples are bleached on the surface. A chemical analysis by XPS is in progress to verify if this white compound would be PbBr<sub>2</sub>. In a thick layer, it has been shown that this mechanism would be reversible as long as the loss of dibromium Br<sub>2</sub> in the environment remains limited<sup>1</sup>. Nevertheless, it is possible that the action of oxygen compensates the creation of defects linked to the photodegradation reaction.



X-ray induced photocurrent measurements were made on a sample slice in order to evaluate the electric field and its drift over time. The environment of the cell, including many motors, brought a lot of electromagnetic disturbance and noise on the measurements, but experimental conditions (cable shielding) have been found for the measurements. Another difficulty came from the drift of the dark current (intrinsic to the materials) that

<sup>1</sup> <https://onlinelibrary.wiley.com/doi/10.1002/adma.201706273>

<sup>2</sup> J. Phys. Chem. C, <https://pubs.acs.org/doi/10.1021/acs.jpcc.7b12740>

<sup>3</sup> ACS Appl. Mater. Interfaces, <https://doi.org/10.1021/acsami.1c16072>

masked the photocurrent. Home-made LabVIEW program was developed to handle the .h5 format of the data. The first acquisition with an applied voltage of -15V (red curve Figure 3) showed a decreasing electric field close to the right electrode.

However, from the second series of measurements, a shutter fault on the light line suppressed the X-ray beam.

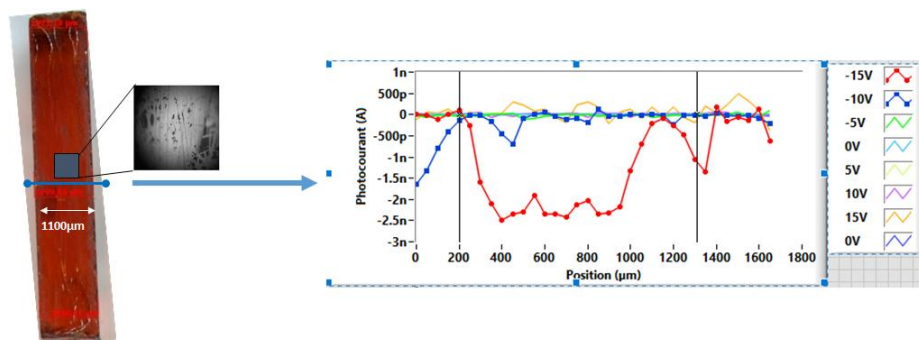


Figure 3: X-ray induced photocurrent (XBIC) as a function of the irradiation position for different applied voltages. The theoretical positions on the two electrodes are represented by the two black lines

X-ray fluorescence measurements did not evidence a good contrast to image change of composition in these samples.

In conclusion, in spite of a significant effort, these measurements at ESRF did not allow us to improve our understanding of the mechanisms related to the movements of the ions under the effect of the applied electric field. Complementary XBIC and XRF measurements should be made to prove that the dark current drift is due to the movement of ions, including halide ions.